

PHOTOCATALYTIC ACTIVITY OF MN-N CO-DOPED ZNS NANOPARTICLES FOR DEGRADATION OF ORGANIC POLLUTANT (METHYLENE BLUE)**Dagim Zewdie Zegeye¹, Dr. O.P.Yadav¹ and Abi Tadesse Mengesha²**¹Associate professor, Department of Chemistry, Faculty of Natural and Computational Science, Haramaya University, Dire Dawa, Ethiopia²Professor, Department of Chemistry, Faculty of Natural and Computational Science, Haramaya University, Dire Dawa, Ethiopia

ABSTRACT: *Nanoparticles of undoped ZnS, Mn-doped-ZnS, N-doped-ZnS and Mn-N co-doped ZnS were prepared by using chemical co-precipitation method. The precursors used to synthesize the photocatalyst nanoparticles were: Zn(CH₃COO)₂·2H₂O, Mn(CH₃COO)₂·4H₂O and Na₂S·9H₂O. The characterization of nanoparticles was done using X-ray powder diffraction (XRD) and UV–VIS Spectrophotometric technique. The average crystalline size of as-synthesized photocatalysts calculated using the Debye-Scherrer formula was 7.80, 7.48, 6.61 and 6.59 nm for Zc, NZ, MZ, and MNZ respectively. The percentage degradation of methylene blue under UV irradiation at 180 minutes were: 10.12, 24.85, 45.19, 38.09, and 55.60 for uncalcined zinc sulfide (Zc), calcined zinc sulfide (Zc), Mn-doped zinc sulfide (MZ), N-doped zinc sulfide (NZ) and Mn-N co-doped zinc sulfide (MNZ) respectively. Under solar irradiation the Percentage photodegradation of MB were: 13.53, 30.17, 49.00, 57.30 and 70.75 for Zc, Zc, MZ, NZ, and MNZ respectively. The pseudo first order rate constant (k) of MB photodegradation for Zc, Zc, NZ, MZ, and MNZ were 5.72×10^{-4} , 1.64×10^{-3} , 2.54×10^{-3} , 3.23×10^{-3} and $4.48 \times 10^{-3} \text{ min}^{-1}$ and 0.8×10^{-3} , 2.15×10^{-3} , 4.16×10^{-3} , 5.3×10^{-3} and $8.66 \times 10^{-3} \text{ min}^{-1}$ under UV irradiation and under solar irradiation, respectively.*

KEYWORDS: Chemical co-precipitation, Degradation, Photocatalysis, Rate constant, XRD

INTRODUCTION

Organic dyes are one of the major groups of pollutants in waste waters released from textile and other industrial processes (Hun *et al.*, 1999; Kiwi *et al.*, 1993 and Li *et al.*, 2004). Over 15% of the textile dyes are lost in wastewater stream during dyeing operation. The textile industry produces large quantity of high colour effluents, which are generally toxic and resistant to degradation by biological treatment methods. A necessary criterion for the use of these dyes is that they must be highly stable towards light and during washing. They must also be resistant to microbial attack. Therefore, dyes in waste water are not readily degradable and are not easily removed from water by conventional chemical treatment systems (Tang *et al.*, 1995). Among various physical, chemical and biological techniques for treatment of wastewaters, heterogeneous photocatalysis has been considered as a cost-effective alternative for water remediation (Hoffman *et al.*, 1995).

Recently, use of nanosize semiconductors photocatalytic oxidation to toxic pollutants is being increasingly valued. A lot of organic matter can be decomposed into inorganic and less toxic simpler compound. Because, this kind of reaction needs only light, catalyst and air, the processing cost is lower, thus becoming a new promising method for waste water treatment (Legrini *et al.*, 1993; Hu *et al.*, 1995).

Several semiconductor photocatalysts being used for the treatment of waste water pollutants are: TiO₂, ZnO, WO₃, SnO₂, CdS and ZnS (Herrmann, 1999). In particular TiO₂ has drawn much attention in research and industrial fields in recent years because of its characteristic powerful oxidation capability, non-toxicity, chemical stability, and cost-effectiveness.

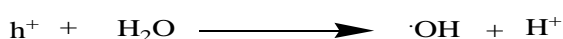
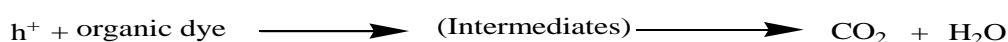
In other words, semiconductor materials are materials whose valence band and conduction band are separated by an energy gap or band-gap. When a semiconductor molecule absorbs photons with energy equal or greater than its band-gap, electrons in the valence band can be excited and jump up into the conduction band, and thus charge carriers are generated. In order to have a photocatalyzed reaction, the e⁻-h⁺ recombination, subsequent to the initial charge separation, must be prevented as much as possible (Gerven *et al.*, 2007).

Co-doping of metal-non-metal may further improve photocatalytic activities of ZnS by reducing anodic photo-corrosion, improving its stability in acidic or basic solutions, further narrowing of the band gap energy of zinc Sulfide and minimizing electron-hole recombination.

Principles of Photocatalytic Oxidation

In the photocatalyst oxidation process, organic pollutants are destroyed in the presence of semiconductor photocatalyst an energetic light source and an oxidizing agent such as oxygen or air. Only photons with energies greater than the band-gap energy can result in the excitation of valence band (VB) electrons which then promote the possible reactions with organic pollutants. The absorption of photons with energy lower than the band-gap energy or longer wavelengths usually causes energy dissipation in the form of heat. The illumination of the photocatalyst with sufficient energy leads to the formation of a positive hole (h⁺) in the valence band and an electron (e⁻) in the conduction band (CB). The positive hole oxidizes either the pollutant directly or water to produce hydroxyl radical ·OH, whereas the electron in the conduction band reduces the oxygen adsorbed on the photocatalyst (Ahmed *et al.*, 2010).

Oxidative reaction:

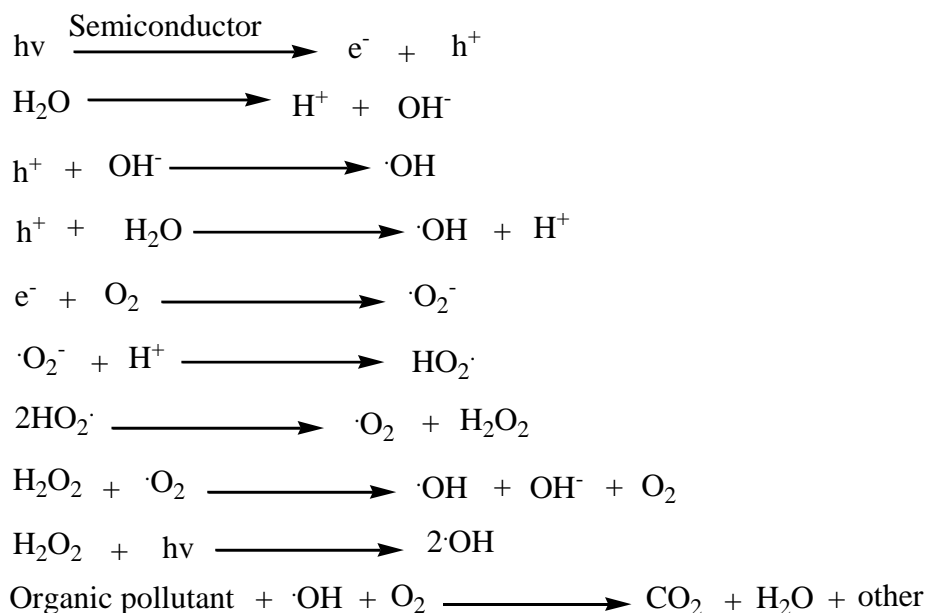


Reductive reaction:



Hydroxyl radical generation by the photocatalytic oxidation process is shown in the above steps. In the degradation of organic pollutants, the hydroxyl radical generated from the oxidation of adsorbed water is the primary oxidant, and the oxygen present reacts with electron at the conduction band to form peroxide radicals followed by a number of steps forming H₂O₂ or ·OH radical thus can prevent the recombination of an electron-hole pair. The ·OH attacks organic compounds resulting in various reaction intermediates depending on the nature of the compounds. The resulting intermediates further react with ·OH to produce final degradation products such as CO₂ and H₂O. In the photocatalytic degradation of pollutants, when the reduction process of oxygen and the oxidation of pollutants do not advance simultaneously, there is an electron accumulation in the CB, thereby causing an increase in the rate of recombination of e⁻ and h⁺ (Hoffmann *et al.*, 1995; Herrmann, 1999).

The basic reactions of above mentioned process are as follows: (Cuiet *al.*, 2001 and Lei, 2001).



EXPERIMENTAL

Preparation of zinc sulfide nanoparticles

Zinc acetate dihydrate ($\text{Zn}(\text{CH}_3\text{COO})_2 \cdot 2\text{H}_2\text{O}$), 1M of 100 ml and 100 ml of 1M solution of sodium sulphide were mixed at 80 °C using magnetic stirrer and 100 ml of ethanol was added with stirring. Then 30 ml of deionized water containing 2g of EDTA was added drop by drop and the process was continued for two hours. After 2 hours, the solution was cooled at room temperature (Murugadosset *al.*, 2009). The precipitate was washed at several times using distilled water and alcohol to remove the impurities, if any. Finally the wet precipitate was dried in hot air oven and labeled as uncalcined zinc sulfide (Znc). Some portion of the product (Znc) was calcined at 350°C for 2hrs, cooled to room temperature, ground in agate mortar and labeled as calcined zinc sulfide (Zc).

Preparation of manganese-doped zinc sulfide

Zinc acetate dihydrate ($\text{Zn}(\text{CH}_3\text{COO})_2 \cdot 2\text{H}_2\text{O}$) 1M of 50 ml, 10 ml of 0.1M solution of manganese acetate and 50 ml of 1M solution of sodium sulphide were mixed at 80 °C using magnetic stirrer. Then 100 ml of ethanol was also added during stirring. Then 15 ml of deionized water containing 1g of EDTA was added drop by drop and the process was continued for two hours. After 2 hours, the solution was cooled at room temperature (Murugadosset *al.*, 2009). The precipitate was separated from the mixture several times using distilled water and alcohol to remove the impurities, including traces of EDTA and the original reactants, if any. Finally the wet precipitate was dried in hot air oven and the powder was cooled to room temperature. The dried powder was calcined at 350°C for 2 hrs, ground in agate mortar and the obtained product was labeled as manganese-doped zinc sulfide (MZ).

Preparation of nitrogen-doped zinc sulfide

5g of Zinc sulfide was added to 15 g of urea, ground in an agate mortar and mixed well. The mixture was calcined in a ceramic crucible at 350⁰C for 2 hrs, cooled to room temperature and was ground in an agate mortar (Zheng & Wu, 2009). The product was labeled as nitrogen-doped zinc sulfide (NZ).

Preparation of Manganese-nitrogen co-doped zinc sulfide

5 g of manganese-doped-zinc sulfide (MZ) was added to 15 g of urea, ground in an agate mortar and mixed well. The mixture was calcined in a ceramic crucible at 350⁰C for 2 hrs, cooled to room temperature and was ground in an agate mortar. The product was labeled as manganese-nitrogen-co-doped zinc sulfide (MNZ).

Photocatalytic degradation studies

Photocatalytic degradation of methylene blue (MB) was carried out using a reactor consisting of a glass tube with an inlet tube for provision of air purging during photocatalysis and outlet for the collection of samples from the reactor at different time intervals. A 0.15g of the as-synthesized photocatalyst powder and 500 ml aqueous solution of methylene blue of known concentration was taken in the reactor tube and the suspension was stirred in dark for 40 minutes to obtain adsorption/desorption equilibrium before irradiating the dye. 10 ml of the sample was withdrawn at 20 minutes regular time interval. The suspension was centrifuged at 2500 rpm for 5 minutes and filtered to remove the catalyst particles before measuring absorbance. The absorbance of the clear solution was measured at $\lambda_{\max} = 665 \text{ nm}$ using UV/Vis spectrophotometer (SP65) for quantitative analysis. The degradation efficiency of MB has been calculated as (Pouretedal *et al.*, 2009).

$$\% \text{ Degradation} = [(C_0 - C) / C_0] \times 100\% \dots \dots \dots (1)$$

Where C_0 is the initial concentration of MB and C is the concentration of MB after irradiation at a given time.

RESULT AND DISCUSSION

XRD analysis

In the XRD pattern of Zinc sulfide (Fig.1) there were three diffraction peaks at $2\theta = 28.66^\circ$, 47.56° and 56° which correspond to (111), (220) and (311) planes of the cubic crystalline ZnS (Pedro *et al.*, 2006). Due to size effect, the XRD peaks were broadened and their widths become larger as the particles become smaller. The obtained XRD results were very well matched with the standard cubic ZnS. The XRD peaks of the cubic crystallite Zinc sulfide nanoparticles proved to be broad due to small particle size (Pedro *et al.*, 2006). The broadness of peaks indicates the formation of nanoparticles and sharp peaks indicates the crystalline nature of the materials.

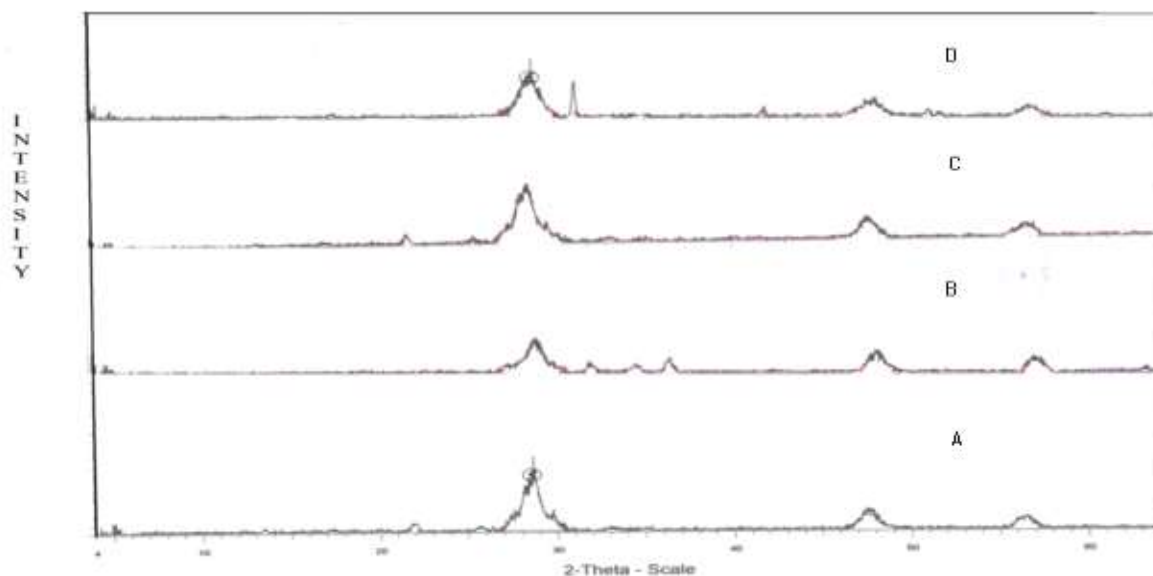


Figure 1. XRD spectra (A) Calcined ZnS, (B) Mn-doped ZnS , (C) N-doped ZnS , and (D) Mn-N codoped ZnS

On doping Mn-in zinc sulfide and Mn-N-co-doped zinc sulfide an additional peak at $2\theta = 31.2^\circ$ (compare Fig.2B and 2D) is observed suggesting distortion of ZnS cubic structure to partial tetragonal structure. Based on the observed full width at half maximum (FWHM) value of the (111) peak and using Debye-Scherrer formula the average particle size were calculated from equation (2) and recorded in (Table 1).

$$D = 0.9\lambda/\beta \cos\theta \text{ (Wu, 2004)} \dots \dots \dots (2)$$

Where D is the average crystallite size, λ is the wavelength of the X-ray = 0.15406 nm for Cutarget $K\alpha$ radiation, β is the full width at half maximum of an XRD peak and θ is the Bragg's angle. The average crystallite size (D) of the photocatalysts is given in table 1.

Sample	2θ (Degree)	β (Radian)	D (nm)
Zc	28.66	0.0183	7.80
NZ	28.87	0.0191	7.48
MZ	28.57	0.0216	6.61
MNZ	28.71	0.0211	6.59

UV/Vis diffuse absorption measurements

The optical absorption spectra of photocatalysts i.e. Zinc Sulfide, Mn-doped Zinc Sulfide, Nitrogen doped Zinc sulfide, and Mn-N-co-doped Zinc sulfide measured in the UV-Vis region are shown below in Figures 3-6. Absorption edge for ZnS, Mn-ZnS, N-ZnS and Mn-N-ZnS are: 336, 334, 385 and 400 nm, respectively.

For Mn-dopedzinc sulfide absorption edge shifted to a higher energyas compared to the pure ZnS sample due to quantum confinement effect(Yanget *al.*, 2001). The blue shift in the

absorption spectrum edge is a clear indication for the incorporation of dopant inside the ZnS lattice (Srideviet *al.*, 2010)

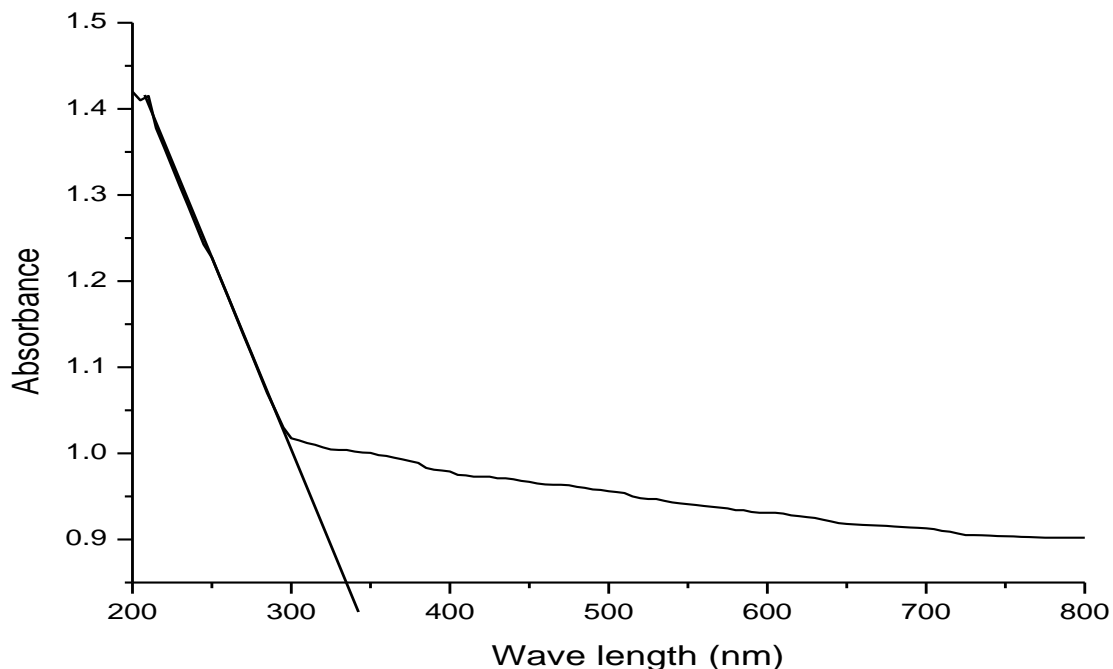


Fig2. UV-Visible absorption spectra of calcined zinc sulfide (absorption edge 336 nm)

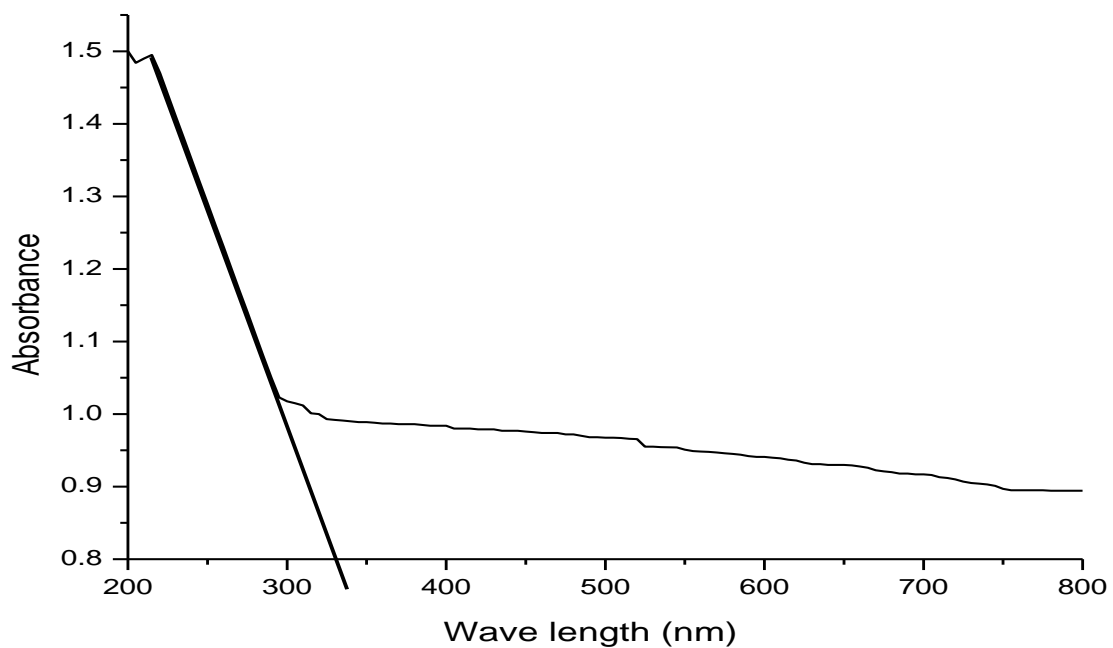


Figure 3. UV-Visible absorption spectra of Mn- zinc sulfide (absorption edge 334 nm)

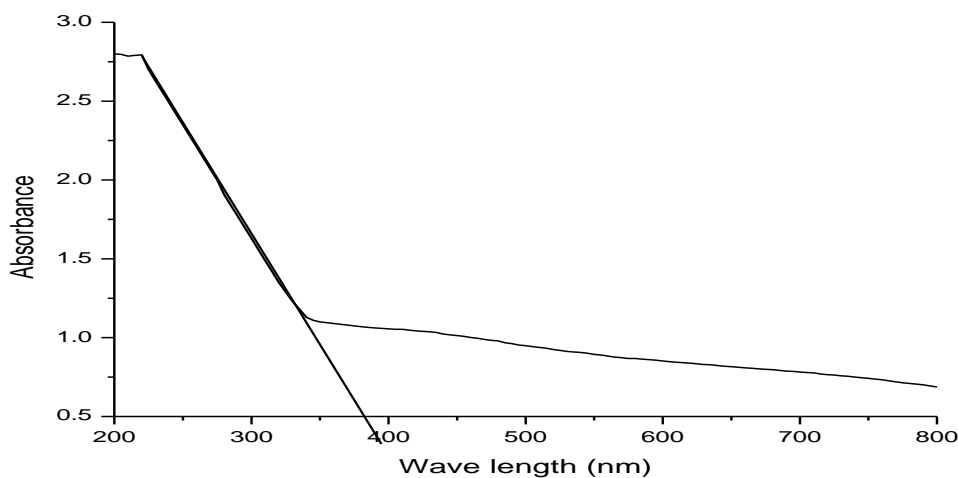


Fig4. UV-Visible absorption spectra of N- doped zinc sulfide (absorption edge 385 nm)

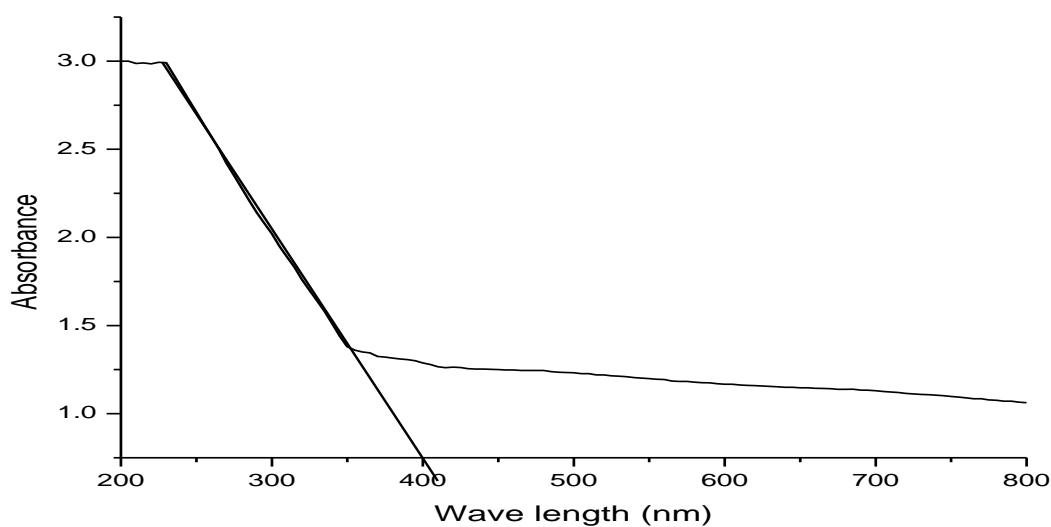


Fig5. UV-Visible absorption spectra of Mn-N-co-doped zinc sulfide (absorption edge 400 nm)

Band gap energy of the as-synthesized photocatalysts was obtained using the relation (El-Kemary *et al.*, 2009).

$$E_g \text{ (eV)} = hc/\lambda = [1240\text{eV nm} / \lambda] \dots\dots\dots(3)$$

The band gap energies (E_g) of photocatalysts Zc, MZ, NZ, and MNZ were found as 3.69, 3.71, 3.22, 3.10 eV, respectively.

Photocatalytic Degradation Study

The plots of percentage adsorption/degradation of methylene blue as a function of time under no irradiation, UV irradiation and solar irradiation are shown from Fig.7-9. The rate of decolorization was recorded with respect to the change in intensity of absorbance at 665 nm.

The percentage adsorption of MB without irradiation using the adsorbents: Znc, Zc, MZ, NZ, and MNZ at 180 minutes were: 0.55, 1.50, 2.40, 2.21 and 2.50 respectively (Fig. 8). The percent adsorption of MB in dark are used as reference as zero minute irradiations (Patil *et al.*, 2010). The percentage photodegradation of MB for Znc, Zc, MZ, NZ and MNZ under UV irradiation are: 10.12, 24.85, 45.19, 38.09, and 55.60 respectively at 180 minutes (Fig.9) and such values under solar irradiation are: 13.53, 30.17, 49.00, 57.30 and 70.75 respectively (Fig.10).

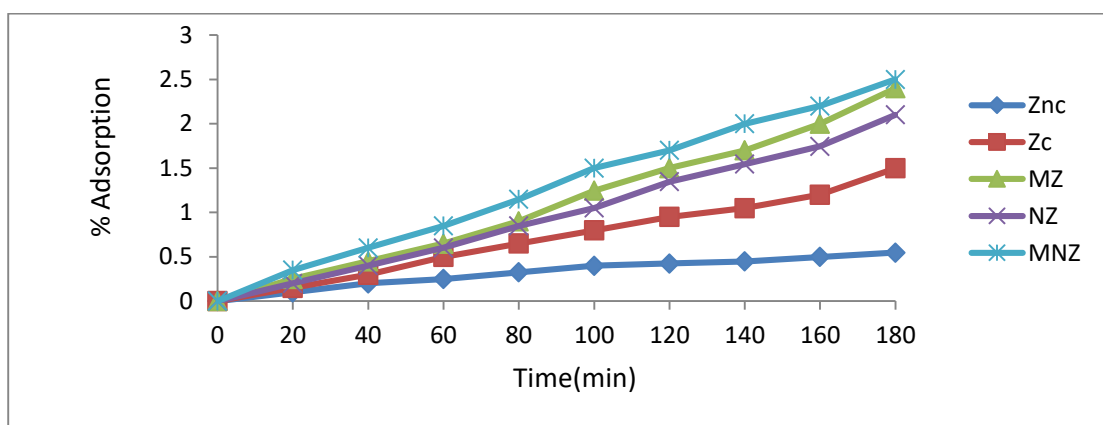


Figure 6. Plots of percentage adsorption of MB as a function of time (without irradiation)

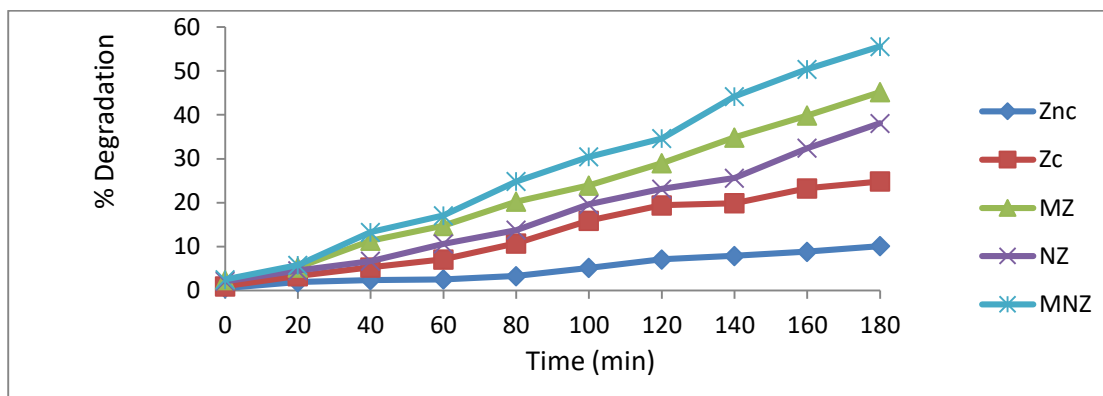


Figure 7. Plots of percentage degradation of MB as function of time (under UV irradiation)

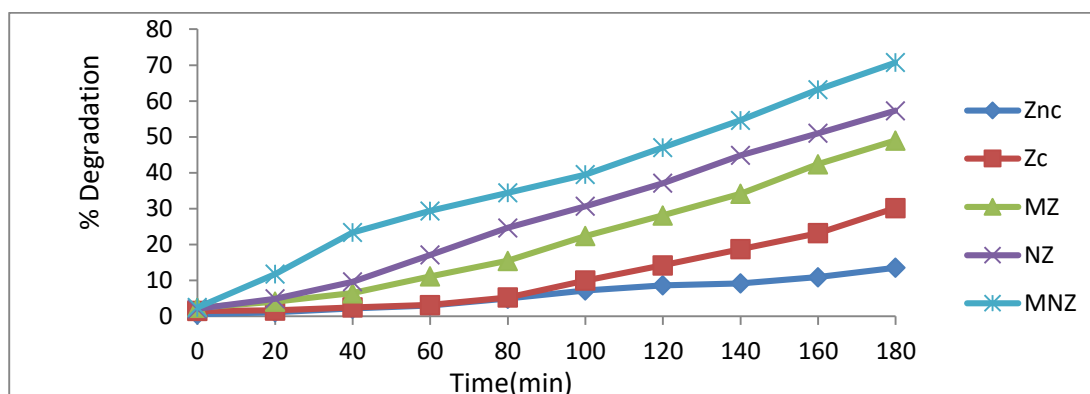


Figure 8. Plots of percentage degradation of MB as function of time (under solar irradiation)

Note: Znc: uncalcined zinc sulfide, Zc: calcined zinc sulfide, MZ: Mn-doped zinc sulfide, NZ :N-doped zinc sulfide and MNZ: Mn-N co-doped zinc sulfide

The photocatalytic activity of MNZ is highest among all the studied photocatalysts under both solar as well as UV irradiations. It may be due to the synergetic cumulative effect of manganese and nitrogen co-doping.

Kinetic Studies of Photocatalytic Degradation of MB

The kinetics behavior of photocatalytic reaction can be described by a modified Langmuir-Hinshelwood model (Zhang *et al.*, 1998 and Fu *et al.*, 2005). The kinetics adsorption/photodegradation of MB for an initial concentration of 25 mg/l show that the photocatalytic decolorization of dye can be described by the first order kinetics (eq.5).

$$\ln(C_0/C) = kt \dots \dots \dots (5)$$

Where C_0 is the initial concentration of MB and C is its concentration at any time, t

The rate constant for adsorption of MB without irradiation using the adsorbents: Znc, Zc, MZ, NZ, and MNZ are: 0.95×10^{-4} , 1.17×10^{-4} , 1.28×10^{-4} , 1.39×10^{-4} and $1.39 \times 10^{-4} \text{ min}^{-1}$ respectively (Fig.11). The rate constants (k) for the degradation of MB, using Znc, Zc, NZ, MZ and MNZ under UV irradiations: 5.72×10^{-4} , 1.64×10^{-3} , 2.54×10^{-3} , 3.23×10^{-3} and $4.48 \times 10^{-3} \text{ min}^{-1}$ for respectively (Fig.12). Under solar irradiation the rate constants of dye degradation were: 0.8×10^{-3} , 2.15×10^{-3} , 4.16×10^{-3} , 5.3×10^{-3} and $8.66 \times 10^{-3} \text{ min}^{-1}$ (Fig.13). These results again suggest the synergetic effect of co-doping Mn and N into ZnS towards enhancing the photocatalytic activity of ZnS.

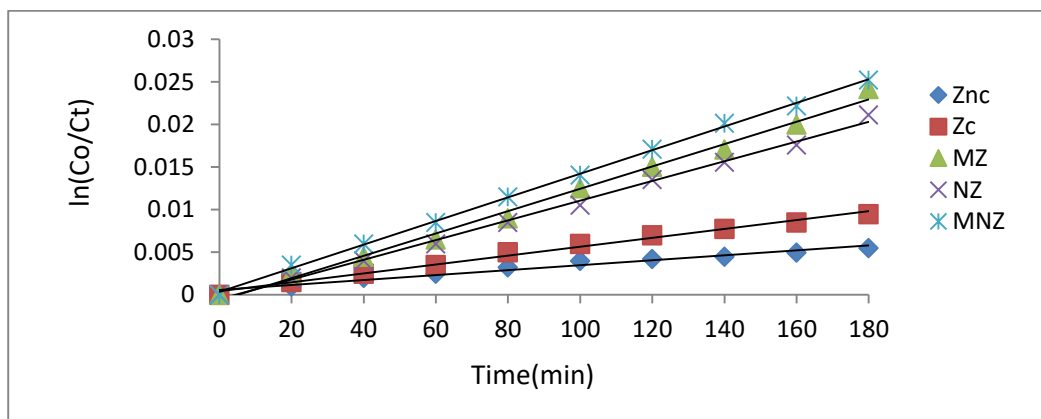


Figure 9. Plot of $\ln(C_0/C_t)$ vs. time curves for photocatalytic degradation of MB using zinc sulfide and modified zinc sulfide photocatalysts (without irradiation)

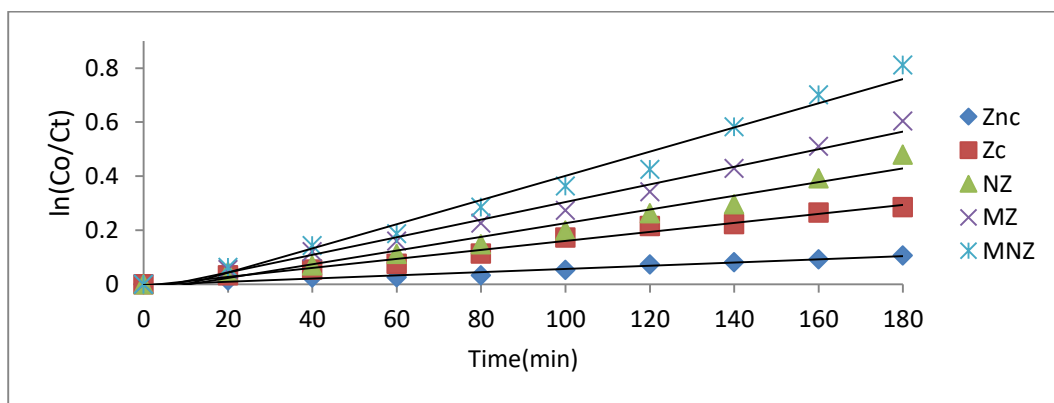


Figure 10. Plot of $\ln(C_0/C_t)$ vs. time curves for photocatalytic degradation of MB using zinc sulfide and modified zinc sulfide photocatalysts (under UV irradiation)

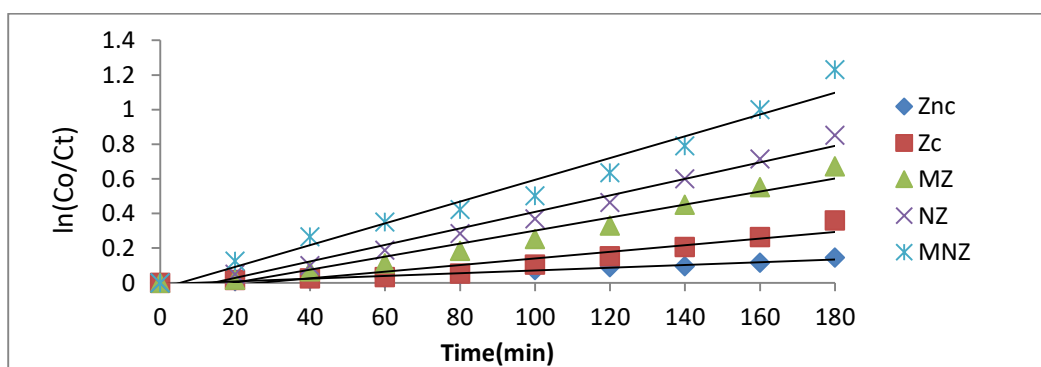


Figure 11. Plot of $\ln(C_0/C_t)$ vs. time for photocatalytic degradation of MB using zinc sulfide and modified zinc sulfide photocatalysts (under solar irradiation)

SUMMARY AND CONCLUSION

Zinc sulfide, Mn-doped zinc sulfide, N-doped zinc sulfide and Mn-N co-doped zinc sulfide photocatalyst nanoparticle have been synthesized. The characterization of nanoparticles was done using X-ray powder diffraction (XRD) and UV–VIS Spectroscopy.

XRD results reveal that doped Mn merely adheres at the surface of ZnS, but N-doped in ZnS replace some of S atom in the crystal lattice and thus distorts the ZnS cubic structure. Manganese and Nitrogen co-doping into ZnS exhibited synergetic effect towards enhancing its photocatalytic activity. Whereas Mn doped ZnS entraps the photo-excited electron at the conduction band of ZnS thereby minimizing electron-hole recombination. Nitrogen doped in ZnS extends the photo-absorption in the visible range.

The photocatalytic activity of Mn-N co-doped ZnS is highest among the studied photocatalysts under both solar as well as UV irradiations. It may be due to the synergetic cumulative effect of manganese and nitrogen co-doping in enhancing the photocatalytic activity. The results also indicate that decolorization of methylene blue using N-doped ZnS occurs at a fast rate with solar light in comparison to UV radiation. Maximum decolorization 70.75% was observed at 180 min under solar light. Under UV irradiation the decolorization was only 55.60 %.

The photocatalytic degradation of methylene blue using as synthesized photocatalysts follows pseudo-first order kinetics. Since correlation coefficient $R^2 > 0.96$ it was found that all reactions were found to follow a pseudo-first-order kinetics. The order of photocatalytic efficiency of as-synthesized nanomaterials under solar irradiation is: MNZ > NZ > MZ > Zc > Znc and at the same time under UV irradiation MNZ > MZ > NZ > Zc > Znc.

Acknowledgements

We are grateful to Haramaya University and Ministry of education for providing financial support to undertake this work.

REFERENCES

- Ahmed, S., M.G. Rasul, R. Brown and M.A. Hashib, 2010. Influence of parameters on the heterogeneous photocatalytic degradation of pesticides and phenolic contaminants in wastewater. *J. Environ. Manag.* 9: 311- 330.
- Cui, Y., Z. Yiren and H. Dongbao, 2001. A Study on Treatment of Papermaking Wastewater by $WO_3/\alpha-Fe_2O_3/W$ as Heterogeneous Photocatalyst. *Photographic Science and Photochem.* 19(2): 131-138.
- El-Kemary, M. and H. El-Shamy, 2009. Fluorescence modulation and photodegradation characteristics of safranin o dye in the presence of zns nanoparticles. *J. Photochem. and Photobiol. A: Chem.* 205: 151–155.
- Fu, H., C. Pan, W. Yao and Y. Zhu, 2005. Visible light induced degradation of rhodamine B by nanosized Bi_2WO_6 . *J. Phys. Chem. B.* 109:2434-2439.
- Gerven, T.V., G. Mul, J. Moulijn and A. Stankiewicz, 2007. A review of intensification of photocatalytic processes. *Chem. Eng. Proc.* 46: 781–789.
- Herrmann, J.M., 1999. Heterogeneous photocatalysis: fundamentals and applications to the removal of various types of aqueous pollutants. *Catalysis Today.* 53: 115-129.

- Hoffmann, M.R., S.T. Martin, W. Choi and D.W. Bahnemann, 1995. Environmental applications of semiconductor photocatalysis. *Chem. Rev.* 95: 69–96.
- Hu, C., W. Yizhong and T. Hongxiao, 1995. The Theory and Application Progress of the Multiphase Photocatalytic Oxidation Technologies. *Progress in Environ. Science.* 3(1): 55.
- Hun, C. and Y.Z. Wang, 1999. Decolorization and biodegradability of photocatalytic treated azo dyes and wool textile wastewater. *Chemosphere.* 39: 2107–2115.
- Kiwi, J., C.M. Pulgarine and P.P. Gratzel, 1993. Beneficial effects of homogeneous photo-Fenton pretreatment upon the biodegradation of anthraquinone sulfonate in waste water treatment. *Appl. Catal. B.: Environ.* 3: 85–99.
- Legrini, O., E. Oliveros and A.M. Braun, 1993. Photochemical Processes for Water Treatment. *Chem Rev.* 93(2): 671-698.
- Lei, L. and W. Dacui, 2001. Wastewater Treatment Technology of Advanced Oxidation. Beijing: Chemical Industry Press. 252-255.
- Li, J., Y. Xu, Y. Liu, D. Wu and Y. Sun, 2004. Synthesis of hydrophilic ZnS nanocrystals and their application in photocatalytic degradation of dye pollutants. *Chin. Particuol.* 2: 266–269.
- Murugadoss G., B. Rajamannan, U. Madhusudhanan, 2009. synthesis and characterization of water-soluble ZnS: Mn²⁺ nanocrystals. *Chalcogenide Letters.* 6(5): 197 – 201.
- Patil, A.B., K.R. Patil and S.K. Pardeeshia, 2010. Ecofriendly synthesis and solar photocatalytic activity of S-doped ZnO. *J. Hazard. Mater.* 183: 315-323.
- Pedro, A., B. Gonzalez, B.R. McGarvey, B.O. Skadtchenko, S. Muralidharan and R.C.W. Sung, 2006. Structural analysis of zinc sulphide nanoparticles synthesized via wet chemical route. *J. Nanoparticle Research.* 8: 235-241.
- Pouretedal, H.R., A. Norozi, M.H. Keshavarz and A. Semnani, 2009. Nanoparticles of zinc sulfide doped with manganese, nickel and copper as nanophotocatalyst in the degradation of organic dyes. *J. Hazard. Mater.* 162: 674–681.
- Sridevi, D. and K.V. Rajendran, 2010. Enhanced Photoluminescence Of ZnS Nanoparticles Doped With Transition and Rare Earth Metallic Ions. *J. Chalcogenide Letters.* 7: 397-401.
- Tang, W.Z. and H. An, 1995. Photocatalytic degradation kinetics and mechanism of acid blue 40 by TiO₂/UV in aqueous solution. *Chemosphere* 31: 4171–4183.
- Wu, C.H., 2004. Comparison of azo dye degradation efficiency using UV/single semiconductor and UV/coupled semiconductor systems. *Chemosphere.* 57: 601-608.
- Yang, P., M. Lu, D. Xu, D. Yuan and G. Zhou, 2001. ZnS Nanocrystals Co-Activated By Transition Metals and Rare-Earth Metals-A New Class of Luminescent Materials. *Journal of Luminescence.* *J.Lumin.* 93: 101
- Zhang, F.L., J.C. Zhao, T. Shen, H. Hidaka, E. Pelizzetti and N. Serpone, 1998. TiO₂-assisted photodegradation of dye pollutants II Adsorption and degradation kinetics of eosin in TiO₂ dispersions under visible light irradiation. *J. Appl. Catal. B: Environ.* 15: 147-156.
- Zheng M. and J. Wu, 2009. One-step synthesis of nitrogen-doped ZnO nanocrystallites and their properties. *Appl. Sur. Sci.* 255: 5656–5666.